

Power dependence of density limit due to plasma-wall interaction in a burning plasma

Jiaxing Liu¹, Ping Zhu^{1,2*}, Dominique Franck Escande³

¹State Key Laboratory of Advanced Electromagnetic Technology, International Joint Research Laboratory of Magnetic Confinement Fusion and Plasma Physics, School of Electrical and Electronic Engineering, Huazhong University of Science and Technology, Wuhan, 430074, China.

²Department of Nuclear Engineering and Engineering Physics, University of Wisconsin-Madison, Madison, Wisconsin, 53706, United States of America.

³Aix-Marseille Université, CNRS, PIIM, UMR 7345, Marseille, France.

E-mail: zhup@hust.edu.cn

20 February 2025

Abstract. The density limit is one of the major obstacles to achieving the desired fusion performance in tokamaks. However, the underlying physics mechanism for its recently observed power dependence in experiments has not been well understood or predicted in theory. In this work, the power dependent scalings of density limit are obtained based on the plasma-wall self-organization theory [D.F. Escande 2022 NF], which are able to match the power dependence of density limits in multiple tokamak devices. The key factors influencing the power dependence are found to be the plasma-wall sputtering and the particle confinement time. The effects of non-sputtered impurities and fusion products are further evaluated. This PWSO-density limit model is then extended to the burning plasma regime and used to predict the conditions for entering burning plasma.

Keywords: Density limit, impurity radiation, plasma-wall interaction, burning plasma condition

1. Introduction

The operation of tokamak often terminates due to disruptions above an upper limit on plasma density n_e [1, 2], which significantly constrains the tokamak performance and ultimately influences its ability to achieve fusion ignition. Experimentally, the well known Greenwald scaling law for density limit (DL) $n_G (10^{20} \text{m}^{-3}) = I_p (\text{MA}) / \pi a (\text{m})^2$ has been established for decades, where I_p is the plasma current and a is the minor radius [1, 2]. However, many experiments demonstrate that the density limit increases with the heating power [3] in various devices, such as JT-60[4], ASDEX-U[5, 6] and TEXTOR-96[7], where the exact power scalings differ in different heating regimes. For instance, DL is proportional to (independent of) heating power at lower (higher) heating power regime as shown in the Fig. 10 of Ref. [8].

Many experiments suggest that the density limit may be attributed to the cooling of tokamak boundary due to impurity radiation [1, 2, 9, 10, 11]. On the other hand, the Greenwald DL scaling is power independent, which is inconsistent with the above scenario of tokamak boundary cooling, because more heating power should be able to suppress or slow down the cooling process and the disruption. Several theoretical models have since been developed to account for the heating power dependence of DL [3, 12, 13, 14, 15, 16, 17, 18, 6]. For example, a power-balance model including the radiation losses from impurities and neutrals is able to predict the power-dependent DL scaling of many L-mode tokamak plasmas $n_c \propto P^{4/9} I_p^{4/9}$ [3], which agrees with a large published data base, where P is the input power to the system.

The recent development of the plasma-wall self-organization (PWSO) theory may provide an alternative and new perspective on the power-dependence of the density limit in tokamak plasmas [19, 20]. In this work, we derive the heating power scaling of density limit due to the plasma wall interaction in a magnetically confined plasma based on the PWSO theory, where the target region plasma temperature T_t depends on the power P_t deposited on the wall, and ultimately the heating power. For the burning plasma regime, the PWSO theory and the corresponding power-dependent DL are applied to re-evaluate the ignition condition as well as the impact from helium ash.

The remainder of this paper is organized as follows: section 2 derives the general power dependent density limit scaling based on 0D PWSO model. Section 3 gives the more specific power-dependent DL scaling based on the particular tokamak regimes, which are compared with experimental results and other theoretical DL scalings. Section 4 evaluate the effect of radiation due to non-sputtered impurities, such as the helium ash from fusion reactions. Section 5 offers a discussion about the effect of plasma-wall interaction on the ignition condition. Lastly, section 6 concludes with a summary and discussion.

2. Effects of heating power on density limit in 0D PWSO model

The effect of heating power on density limit can be derived from the PWSO theory. The plasma-wall self-organization leads to an upper density limit of a tokamak which is related to the sputtering properties of the wall's and target's material [19, 20]. The radiation power due to sputtered impurity at next cycle time is determined by the properties of the wall material and the power deposited on the wall based on the assumption radiation distributes uniformly in the plasma, as shown in following

$$R_+ = \int_V R_{\text{imp,coe}} n_e n_{\text{imp,sputtered}} dV = R_{\text{imp,coe}} n_e \frac{f_{\text{ion}} \lambda a I(T_t)}{2D_{\perp} T_t} P_t = \alpha_1 \frac{I(T_t)}{T_t} P_t \quad (1)$$

$$P_t = P_{\text{heat}} - R \quad (2)$$

where P_t and P_{heat} are the power deposition on wall and the total input power respectively at current cycle time, R and R_+ are total radiation powers due to sputtered impurities at the current and next cycle time respectively, $R_{\text{imp,coe}}$ is the impurity radiation coefficient, and $\alpha_1 = f_{\text{ion}} \lambda n_e R_{\text{imp,coe}} a / (2D_{\perp})$. In the derivation of Eq. (1), the 0D model for the sputtered

impurity density is used [19, 21]

$$n_{\text{imp,sputtered}} = f_{\text{ion}} \lambda P_t I(T_t) / (2\pi a L D_{\perp} T_t) \quad (3)$$

where f_{ion} represents the ionization rate of sputtered neutral impurity, λ the distance between the target/wall and ionization location, a the minor radius, L the toroidal circumference, and D_{\perp} the impurities' particle transport coefficient, $I(T_t)$ is the average of the yield function of carbon $Y(E)$ over the impinging particle energies.

$$I(T_t) = \sqrt{\frac{m}{2\pi T_t}} \int_0^{\infty} Y\left(\frac{mv^2}{2} + \gamma T_t\right) \exp\left(-\frac{mv^2}{2T_t}\right) dv \quad (4)$$

where γ is the total energy transmission coefficient [21], γT_t is a measure of the Debye shield length, and m is the ion mass of impinging particle.

Based on the relation between the target region plasma temperature T_t and the power P_t [21], which we discuss about in detail in section 3, the relation between power P_t and sputtering property $I(T_t)/T_t$ can be established as follows

$$\frac{I(T_t)}{T_t} = \frac{I(T_t(P_t))}{T_t(P_t)} \equiv F(P_t) \quad (5)$$

The steady state of the global power balance in Eq. (1) can be thus written as

$$R_* = \alpha_1 (P_{\text{heat}} - R_*) F \quad (6)$$

The fraction of sputtered impurities is also assumed to have reached a steady state, which is represented by

$$f_{\text{imp}} = \frac{R_*}{n_c^2 R_{\text{coe,imp}}} \quad (7)$$

From the stable condition for the fixed point of Eq. (1)

$$\left| \frac{\partial R_+}{\partial R} \right|_{R=R_*} = \alpha \leq 1 \quad (8)$$

where $\alpha = \alpha_1 [F + (P_{\text{heat}} - R) F']_{R=R_*}$, and $F' = dF/dP_t$. The PWSO density limit n_c can be obtained as follows

$$n_e \leq n_c = \frac{2D_{\perp}}{f_{\text{ion}} \lambda R_{\text{imp,coe}} a} \frac{1}{F + P_t F'} \quad (9)$$

The power dependence of the density limit above mainly comes from the function $F(P_t)$, where P_t relates to the input power P_{heat} through the power balance equation in Eq. (2).

For simplicity, a generic power function is assumed first, i.e. $F(P_t) = \alpha_2 P_t [MW]^{\mu-1}$, which yields a specific form of power dependent density limit as

$$n_e \leq n_c = \frac{2D_{\perp}}{f_{\text{ion}} \lambda R_{\text{imp,coe}} a} \frac{1}{\alpha_2 \mu (P_{\text{heat}} - R_*)^{\mu-1}} = \frac{2D_{\perp}}{f_{\text{ion}} \lambda R_{\text{imp,coe}} a} \frac{P_{\text{heat}}^{1-\mu}}{\alpha_2 \mu \left(\frac{\mu}{\mu+1}\right)^{\mu-1}} \quad (10)$$

where the steady-state relations

$$R_* = \alpha_1 \alpha_2 P_t^\mu, \quad R_* = \frac{P_{\text{heat}}}{\mu + 1}, \quad P - R_* = \frac{\mu}{\mu + 1} P_{\text{heat}} \quad (11)$$

are used. Considering the sputtering of tungsten by deuterium, $R_{\text{imp,coe}} = 10^{-30} \text{Wm}^3$ is estimated based on the simulation results using the FLYCHK code [22], the coefficient α_2 is assumed to be 10^{-5} , $f_{\text{ion}} = 5 \times 10^{-2}$, $\lambda = 10^{-2} \text{m}$, $a = 0.5 \text{m}$, and $D_{\perp} = 1 \text{m}^2 \text{s}^{-1}$. According Eq. (10), the heating power dependence of density limit n_c , which depends on the value of exponent μ , are shown in Fig. 1. The density limit increases (decreases) with the heating power as $\mu < 1$ ($\mu > 1$), and becomes less sensitive to heating power at higher power level. In reality, μ depends on the sputtering property and the relation between the target region plasma temperature T_t and the power deposition on target P_t . Several different μ values observed in experiments can be thus determined based on the specific machine regimes, which we evaluate further in next section.

3. Power dependence of density limit for specific targets

In this section, more realistic functions $F(P_t)$, which is determined by the specific sputtering property in terms of the yield function, and the relation between P_t and T_t , are evaluated to obtain more realistic dependence of density limit on edge power P_t and total heating power P_{heat} .

The relation between edge temperature T_t and edge power P_t can be established theoretically based on 0D particle and energy balance equation (Eq. 4.38 of reference [21])

$$kT_t = P_t \frac{\tau_p}{n_e V} \frac{A_{\Gamma\parallel}}{\gamma A_{q\parallel}} \quad (12)$$

where $k = 1.6022 \times 10^{-19} \text{J/eV}$ is the Boltzmann constant, $V = 2\pi^2 \kappa R a^2$ is the volume, R and a are the major and minor radii respectively, κ is the elongation, γ the sheath heat transmission coefficient, $A_{\Gamma\parallel}$ and $A_{q\parallel}$ are the wet areas of particle and energy flux respectively, and τ_p is the particle confinement time for electrons. The above relation can be integrated with the sputtering function (Eq. (4)) to derive the specific function $F(P_t)$ (Eq. (5)) and the associated power dependence of density limit.

We first take the specific τ_p scaling based on the JET tokamak experimental data $\tau_p [s] \approx 1.3 \times 10^{14} R [m] a [m]^2 (n_e [m^{-3}])^{-0.8}$ [21, 23, 24]. Assuming $\kappa = 1.5$, $\gamma = 7$, $A_{\Gamma\parallel}/A_{q\parallel} = 1$, Eq. (12) can be rewritten as

$$T_t [\text{eV}] = 3.9 \times 10^{30} P_t [\text{W}] (n_e [m^{-3}])^{-1.8} \quad (13)$$

Taking the sputtering of tungsten by deuterium as an example, the function $F(P_t)$ is evaluated based on Eq. (4), Eq. (5) and Eq. (13). Then the dependence of the density limit on the heating power is obtained through Eq. (9) and Eq. (2) as shown in Fig. 2. There are two branches, namely, the high- T_t (>35.5 eV) and the low- T_t (<18 eV) branches, which are fitted to the

scalings $n_c \propto P_{\text{heat}}^{0.255}$ and $n_c \propto P_{\text{heat}}^{0.744}$ respectively. The high- T_i branch scaling $n_c \propto P_{\text{heat}}^{0.255}$ is consistent with the experimental density limit scaling of the tungsten-wall device ASDEX-U $n_c \propto P_{\text{heat}}^\alpha q_{\text{cyl}}^\beta B_{\text{tor}}^\gamma$, where $\alpha \in (0.1, 0.5)$ [6]. The low- T_i density limit scaling, which is in the density free regime in PWSO theory, is relatively higher than the density limit in above and other experiments, such as JET experiment data [25]. The ratio of impurity radiation to heating power $R_{\text{imp}}/P_{\text{heat}}$ for the corresponding two density limit branches also lie on two branches (Fig. 2), where the lower branch of $R_{\text{imp}}/P_{\text{heat}}$ indicates that a relatively small amount of impurity radiation can also lead to density limit disruption. Moreover, in between these two regimes, an intermediate interval exists where n_c decreases with P_{heat} .

Similarly, considering the parameters of ASDEX and W7-AS devices, $T_i[\text{eV}] = 2.5 \times 10^{55} P_t[\text{W}] \bar{n}_{e,\text{main}}^{-3} [\text{m}^{-3}]$ and $T_i[\text{eV}] = 8.0 \times 10^{34} P_t[\text{W}] \bar{n}_{e,\text{main}}^{-2} [\text{m}^{-3}]$ can be obtained by assuming modified τ_p scaling based on JET's (Eq. 13) $\tau_p[\text{s}] \approx 8.3 \times 10^{38} R[\text{m}] a[\text{m}]^2 n[\text{m}^{-3}]^{-2}$ and $\tau_p[\text{s}] \approx 2.66 \times 10^{18} R[\text{m}] a[\text{m}]^2 n[\text{m}^{-3}]^{-1}$ respectively for these two devices. Considering the sputtering of deuterium on boron [26] and $D_\perp = 10^{-2} \text{m}^2/\text{s}$, the theoretical predictions are quantitatively consistent with the ASDEX and W7-AS experimental data from Fig. 20 of [2], the same as Fig. 1 of [26], and the experimental data are located in high- T_i and low- T_i regime of PWSO predictions respectively, as shown in Fig. 3.

The particle confinement time scaling may differ in other and future tokamak devices [23, 27]. For instance, the particle confinement time τ_p based on ohm discharges of DIVE tokamak scales like $\tau_p \propto \sqrt{q_a \bar{n}_e}$, where q_a is the safety factor at edge and $\bar{n}_e [10^{20} \text{m}^{-3}]$ is the line averaged electron density [23, 28]. Thus the corresponding power dependence of density limit may vary as well.

4. Effects of impurity radiation from non-sputtered impurities

In the above analysis, only the impurity radiation from the sputtered impurities is considered. In this section, the radiation due to non-sputtered impurities is also taken into account. The relation between the PWSO density limit n_c and the power P_t in previous section remains the same as in Eq. (9). Compared to the case in absence of radiation effects from non-sputtered impurities, only the power balance becomes different. Additional heating power ΔP_{heat} is required to compensate the radiation power from non-sputtered impurities for the same density limit n_c and the power P_t since

$$P_{\text{heat, without non-sputtered}} = P_t + R_{\text{sputtered}} \quad (14)$$

$$P_{\text{heat, with non-sputtered}} = P_t + R_{\text{sputtered}} + R_{\text{non-sputtered}} \quad (15)$$

$$\Delta P_{\text{heat}} = R_{\text{non-sputtered}} = n_c^2 f_{\text{non-sputtered}} R_{\text{coe, non-sputtered}} \quad (16)$$

where $f_{\text{non-sputtered}} = n_{\text{non-sputtered}}/n_e$ is the fraction level of non-sputtered impurities. Take the non-sputtered carbon fraction $f_{\text{non-sputtered}} = 5\%$ as an example, the heating power dependencies with and without consideration of radiation due to non-sputtered impurity are shown in Fig. 4. Non-sputtered impurity radiation lowers the low- T_i branch of the density limit, whereas the high- T_i branch remains nearly the same.

5. Effects of fusion reactions

In the above discussion, all heating power P_{heat} comes from outside the plasma. For current and future reactors with burning plasma, the effects of fusion reactions, including the α particle heating and radiation due to helium ash may play an important role. In this section, we consider and evaluate the effect of fusion reactions on the heating power dependence of density limit. Similar to the introduction of non-sputtered impurities, the relation between the PWSO density limit n_c and the power P_t remain unchanged for any given specific $F(P_t)$ as in Eq. (9), and only the power balance equation requires modifications due to contributions from fusion reaction products.

The first thing is to assess the fraction of α particles $f_\alpha = f_{\text{He}} = n_{\text{He}}/n_e$. Here we assume an instantaneously and complete thermalization of α -particles out of fusion reactions. The fraction level of sputtered impurities is denoted by $f_{\text{imp}} = n_{\text{imp}}/n_e$. The conservation of Helium particle can be represented as

$$\frac{n_{\text{He}}}{\tau_{\text{He}}} = S_{\text{He}}, \quad S_{\text{He}} = \langle \sigma v \rangle n_T n_D \quad (17)$$

where n_D and n_T are the density of deuterium and tritium, $\langle \sigma v \rangle$ is the fusion reaction rate taken from [29]. Combined with the quasi-neutral condition

$$n_D + n_T + n_{\text{He}} Z_{\text{He}} + n_{\text{imp}} Z_{\text{imp}} = n_e \quad (18)$$

where Z_{He} is the charge number of helium ions, Z_{imp} is the charge number of sputtered impurity ions. The fraction of Helium f_{He} in a plasma with equal proportions of D and T can be determined using Eq. (17) as following

$$n_e f_{\text{He}} = \tau_{\text{He}} \frac{\langle \sigma v \rangle n_e^2}{4} (1 - f_{\text{He}} Z_{\text{He}} - f_{\text{imp}} Z_{\text{imp}})^2 \quad (19)$$

It can be shown there is and only one solution for f_{He} in interval (0,1), which is

$$f_{\text{He}} = \frac{-B - \sqrt{B^2 - 4AC}}{2A} \quad (20)$$

where

$$A = \frac{Z_{\text{He}}^2 \tau_{\text{He}} \langle \sigma v \rangle n_e}{4}, B = -\frac{\tau_{\text{He}} \langle \sigma v \rangle n_e Z_{\text{He}} (1 - f_{\text{imp}} Z_{\text{imp}})}{2} - 1, C = \frac{\tau_{\text{He}} \langle \sigma v \rangle n_e (1 - f_{\text{imp}} Z_{\text{imp}})^2}{4}$$

The dependence of helium fraction f_{He} on the plasma temperature T and impurity fraction f_{imp} determined from Eq. (20) can be evaluated, given the confinement time τ_{He} one second, which is the order required for satisfying the Lawson criterion, in the range of number density and temperature considered in Fig. 5.

The second step is to evaluate the power of α particle heating P_α and helium radiation R_{He} at the PWSO density limit. The helium radiation power is

$$R_{\text{He}} = f_{\text{He}} n_c^2 R_{\text{coe,He}}, \quad P_\alpha = \frac{\langle \sigma v \rangle}{4} U_\alpha n_c^2 (1 - f_{\text{He}} Z_{\text{He}} - f_{\text{imp}} Z_{\text{imp}})^2 \quad (21)$$

where n_c is the density limit as in Eq. (9), f_{He} can be obtained through Eq. (20) for the given plasma temperature T and the fraction level of sputtered impurity f_{imp} governed by Eq. (7). Considering the JET specific scaling for τ_p in Eq. (13) and the corresponding function $F(P_t)$ in Section 3, and calculating the external heating power through the power balance equation as follow.

$$P_{\text{heat}} + P_{\alpha} - R_{\text{imp,sputtered}} - R_{\text{He}} = P_t \quad (22)$$

The density limit power dependence with and without effects of fusion reactions shown in Fig. 6 demonstrate that fusion reactions will enhance the density limit at the same external heating power, which is a result of α particle heating. The effects of fusion reactions are able to enhance the density limit and reduce the needed external heating power to reach the same density limit on the low- T_t branch. However, these effects are very weak on the high- T_t branch. A related discussion about requirements of achieving burning plasma condition as predicted using the 0D PWSO model is presented in Section Appendix A.

6. Summary

In this work, the heating power dependence of density limit in tokamak is explored by considering the plasma-wall interaction through the plasma-wall self-organization theory. The results shows that there are two density limit regimes, low- T_t and high- T_t regions, corresponding to the density-free and density limit regime of the PWSO theory [19, 20], respectively. In particular, in the high- T_t region, the density limit power dependence is about $n_c \propto P_{\text{heat}}^{0.255}$ for the sputtering of tungsten from deuterium and the particle confinement time scaling $\tau_p[s] \approx 1.3 \times 10^{14} R[m] a[m]^2 (\bar{n}_{\text{main}}[m^{-3}])^{-0.8}$ based on the experimental results on JET tokamak. This density limit scaling agree well with the other experimental and theoretical power dependent density limit scaling, especially those listed in Table. 1 of [6]. The low- T_t region's density limit scaling is about $n_c \propto P_{\text{heat}}^{0.744}$ which is much higher than the above DL scaling. Besides, the predictions of this model quantitatively matches experimental trends across devices, including ASDEX-U and W7-AS. The effects of radiation from non-sputtered impurities, and fusion products on the power dependence of density limit are also evaluated. The burning plasma condition under the density limit status is explored and predicted considering the plasma wall interaction. These results underscore the necessity of regulating plasma-wall interactions and confinement properties to achieve higher density limit, offering a pathway toward optimizing performance in next-step fusion reactors.

In future work, we plan to extend the zero-dimensional analysis presented here to higher-dimensional studies using the PWSO theory in 1.5-dimensional integrated simulations, where the effects of various heating schemes, transport mechanisms, and the influence of 1D spatial profiles for electron density, plasma current, and temperature can be taken into account. In addition, cross-machine experiments are proposed on EAST and HL-3 to validate the power dependence scaling of density limit and the role of plasma-wall interaction.

Acknowledgment

This work is supported by the National MCF Energy R&D Program of China under Grant No. 2019YFE03050004 and the U.S. Department of Energy Grant No. DE-FG02-86ER53218. The computing work in this paper is supported by the Public Service Platform of High Performance Computing by Network and Computing Center of HUST.

Appendix A. Burning plasma condition in 0D PWSO model

The energy gain factor $Q = 5P_\alpha/P_{\text{heat}}$ is evaluated for the case in Section 5, and it turns out that the Q value is always much lower than 1 in the temperature ranges in Fig. 7, which means the energy break-even ($Q = 1$) can not be achieved for the JET τ_p scaling in Eq. (13). For a given plasma temperature and density, the α heating power P_α is fixed as in Eq. 21. To reach a higher energy gain factor Q , the relation between n_e , T_t and P_t (Eq. 13)) needs modifications, such as increase the coefficient in front of P_t or increase the exponent of n_e , which would allow a lower power P_t for given electron density n_e and temperature T_t . This is essentially a requirement for the scaling of particle confinement τ_p . Taking the following relation as an example

$$T_t[\text{eV}] = 3.9 \times 10^{30} P_t[\text{W}] (n_e[\text{m}^{-3}])^{-1.745} \quad (\text{A.1})$$

which introduce a slightly different n_e scaling from that in Eq. 13. This scaling will lead to a much higher energy gain factor as shown in Fig. 7.

References

- [1] M. Greenwald, J.L. Terry, S.M. Wolfe, S. Ejima, M.G. Bell, S.M. Kaye, and G.H. Neilson. A new look at density limits in tokamaks. *Nuclear Fusion*, 28(12):2199–2207, 1988.
- [2] M. Greenwald. Density limits in toroidal plasmas. *Plasma Physics and Controlled Fusion*, 44(8):R27–R53, 2002.
- [3] P. Zanca, F. Sattin, D.F. Escande, and JET Contributors. A power-balance model of the density limit in fusion plasmas: application to the L-mode tokamak. *Nuclear Fusion*, 59(12):126011, 2019.
- [4] Y. Kamada, N. Hosogane, R. Yoshino, T. Hirayama, and T. Tsunematsu. Study of the density limit with pellet fuelling in JT-60. *Nuclear Fusion*, 31(10):1827, 1991.
- [5] V. Mertens, M. Kaufmann, J. Neuhauser, J. Schweinzer, J. Stober, K. Buchl, O. Gruber, G. Haas, A. Herrmann, A. Kallenbach, and M. Weinlich. High density operation close to Greenwald limit and H mode limit in ASDEX upgrade. *Nuclear Fusion*, 37(11):1607–1614, 1997.
- [6] P. Manz, T. Eich, O. Grover, and the ASDEX Upgrade Team. The power dependence of the maximum achievable H-mode and (disruptive) L-mode separatrix density in ASDEX Upgrade. *Nuclear Fusion*, 63(7):076026, 2023.
- [7] J. Rapp, P.C. De Vries, F.C. Schüller, M.Z. Tokar, W. Biel, R. Jaspers, H.R. Koslowski, A. Krämer-Flecken, A. Kreter, M. Lehnen, A. Pospieszczyk, D. Reiser, U. Samm, and G. Sergienko. Density limits in TEXTOR-94 auxiliary heated discharges. *Nuclear Fusion*, 39(6):765, 1999.
- [8] A. Huber, M. Bernert, S. Brezinsek, A.V. Chankin, G. Sergienko, V. Huber, S. Wiesen, P. Abreu, M.N.A. Beurskens, A. Boboc, M. Brix, G. Calabrò, D. Carralero, E. Delabie, T. Eich, H.G. Esser, M. Groth, C. Guillemaut, S. Jachmich, A. Järvinen, E. Joffrin, A. Kallenbach, U. Kruezi, P. Lang, Ch. Linsmeier, C.G. Lowry, C.F. Maggi, G.F. Matthews, A.G. Meigs, Ph. Mertens, F. Reimold, J. Schweinzer, G. Sips,

- M. Stamp, E. Viezzer, M. Wischmeier, H. Zohm, and JET contributors. Comparative H-mode density limit studies in JET and AUG. *Nuclear Materials and Energy*, 12:100–110, 2017.
- [9] V. Mertens, W. Junker, M. Laux, M. Schittenhelm, K. Buchl, F. Mast, A. Carlsson, A. Field, C. Fuchs, O. Gehre, O. Gruber, A. Hermann, G. Haas, A. Kallenbach, M. Kaufmann, W. Koppendorfer, K. Lackner, G. Lieder, S. Pitcher, J. Neuhauser, F. Ryter, H. Salzmann, W. Sandmann, K.H. Steuer, M. Weinlich, U. Wenzel, H. Zohm, and ASDEX Upgrade Team. Experimental investigation of marfes and the density limit in the ASDEX upgrade. *Plasma Physics and Controlled Fusion*, 36(8):1307, 1994.
- [10] D.A. Gates and L. Delgado-Aparicio. Origin of tokamak density limit scalings. *Physical Review Letters*, 108:165004, 2012.
- [11] R. Hong, G.R. Tynan, P.H. Diamond, L. Nie, D. Guo, T. Long, R. Ke, Y. Wu, B. Yuan, M. Xu, and The HL-2A Team. Edge shear flows and particle transport near the density limit of the HL-2A tokamak. *Nuclear Fusion*, 58(1):016041, 2017.
- [12] M. Bernert, T. Eich, A. Kallenbach, D. Carralero, A. Huber, P.T. Lang, S. Potzel, F. Reimold, J. Schweinzer, E. Viezzer, H. Zohm, and the ASDEX Upgrade Team. The H-mode density limit in the full tungsten ASDEX Upgrade tokamak. *Nuclear Fusion*, 57(1):014038, 2015.
- [13] T. Eich, P. Manz, and the ASDEX Upgrade Team. The separatrix operational space of ASDEX Upgrade due to interchange-drift-Alfvén turbulence. *Nuclear Fusion*, 61(8):086017, 2021.
- [14] A.O. Brown and R.J. Goldston. Generalization of the Heuristic Drift SOL model for finite collisionality and effect on flow shearing rate vs. interchange growth rate. *Nuclear Materials and Energy*, 27:101002, 2021.
- [15] M. Giacomin, A. Pau, P. Ricci, O. Sauter, T. Eich, the ASDEX Upgrade Team, JET Contributors, and the TCV Team. First-Principles Density Limit Scaling in Tokamaks Based on Edge Turbulent Transport and Implications for ITER. *Physical Review Letters*, 128(18):185003, 2022.
- [16] R. Singh and P.H. Diamond. Zonal shear layer collapse and the power scaling of the density limit: old L-H wine in new bottles. *Plasma Physics and Controlled Fusion*, 64(8):084004, 2022.
- [17] U. Stroth, M. Bernert, D. Brida, M. Cavedon, R. Dux, E. Huett, T. Lunt, O. Pan, M. Wischmeier, and the ASDEX Upgrade Team. Model for access and stability of the X-point radiator and the threshold for marfes in tokamak plasmas. *Nuclear Fusion*, 62(7):076008, 2022.
- [18] P.H. Diamond, R. Singh, T. Long, R.J. Hong, R. Ke, Z. Yan, M.Y. Cao, and G.R. Tynan. How the birth and death of shear layers determine confinement evolution: from the L \rightarrow H transition to the density limit. *Philosophical Transactions of the Royal Society A*, 381(2242):20210227, 2023.
- [19] D.F. Escande, F. Sattin, and P. Zanca. Plasma-wall self-organization in magnetic fusion. *Nuclear Fusion*, 62(2):026001, 2022.
- [20] J.X. Liu, P. Zhu, D.F. Escande, J.L. Zhang, D.H. Xia, Y.H. Wang, J.M. Wang, Q.H. Yang, J.G. Fang, X.Q. Zhang, L. Gao, Z.F. Cheng, Z.P. Chen, Z.J. Yang, Z.Y. Chen, Y.H. Ding, Y. Pan, and the J-TEXT Team. Validation of the plasma-wall self-organization model for density limit in ECRH-assisted start-up of Ohmic discharges on J-TEXT. *Nuclear Fusion*, 63(9):096009, 2023.
- [21] P. C. Stangeby. *The Plasma Boundary of Magnetic Fusion Devices*. CRC Press, 2000.
- [22] H.K. Chung, M.H. Chen, W.L. Morgan, Y. Ralchenko, and R.W. Lee. Flychk: Generalized population kinetics and spectral model for rapid spectroscopic analysis for all elements. *High Energy Density Physics*, 1(1):3–12, 2005.
- [23] S. Tsuji. Experimental scaling of particle confinement in tokamaks. *Fusion Engineering and Design*, 15(4):311–324, 1991.
- [24] S.A. Gohin, J. Ehrenberg, T.T.C. Jones, A. Gondhalekar, M. Bures, P. Coad, L. de Kock, K. Erents, P. Barbour, P.D. Morgan, J. O'Rourke, J.A. Tagle, M. Watkins, and The JET Team. Particle balance and wall pumping in tokamaks. *Plasma Physics and Controlled Fusion*, 29(10A):1205, 1987.
- [25] A. Tanga, K.H. Behringer, A.E. Costley, M. Brusati, B. Denne, A. Edwards, A. Gibson, R.D. Gill, N. Gottardi, and R. Granetz. Magnetic separatrix experiments in JET. *Nuclear Fusion*, 27(11):1877, 1987.
- [26] A. Staebler, R. Burhenn, Peter Eckhard Grigull, J. V. Hofmann, K. McCormick, E. R. Mueller, J. Neuhauser, Dieter Reiter, Ralf Schneider, K. H. Steuer, Arthur Weller, E. Wuersching, Hartmut Zohm, ASDEX-

- team, and WVII-AS-Team. Comparison of density limit physics on the ASDEX tokamak and the Wendelstein 7-AS stellarator. In Plasma Physics and Controlled Nuclear Fusion Research, Wurzburg, Germany, 1993.
- [27] B. Lomanowski, M. Dunne, N. Vianello, S. Aleiferis, M. Brix, J. Canik, I.S. Carvalho, L. Frassinetti, D. Frigione, L. Garzotti, M. Groth, A. Meigs, S. Menmuir, M. Maslov, T. Pereira, C. Perez von Thun, M. Reinke, D. Refy, F. Rimini, G. Rubino, P.A. Schneider, G. Sergienko, A. Uccello1, D. Van Eester, , and JET Contributors. Experimental study on the role of the target electron temperature as a key parameter linking recycling to plasma performance in JET-ILW. Nuclear Fusion, 62(6):066030, 2022.
- [28] DIVE Group. Divertor experiment in DIVA. Nuclear Fusion, 18(12):1619, 1978.
- [29] A.A. Mavrin. New analytic representation of the thermonuclear reaction rates. Plasma Physics and Controlled Fusion, 60(9):092001, 2018.

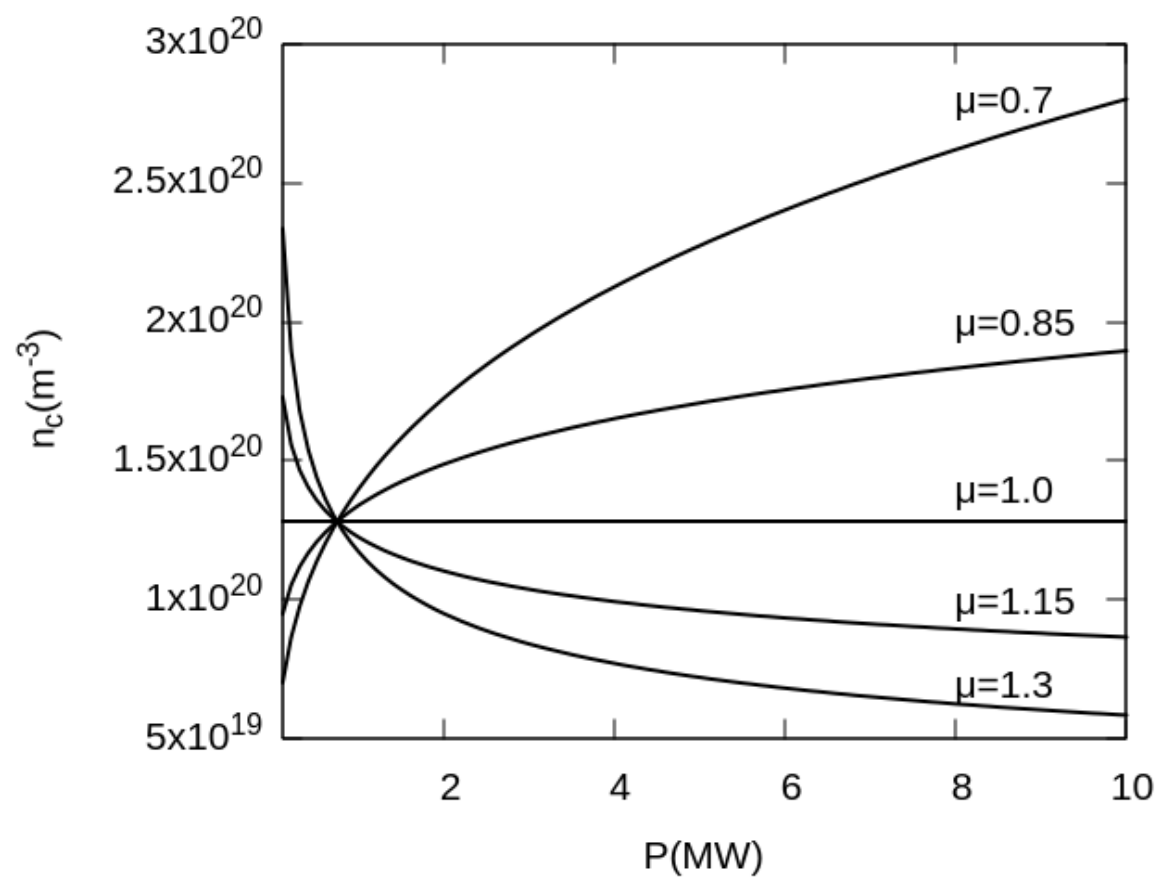


Figure 1. Density limit n_c as functions of the heating power P with various μ values

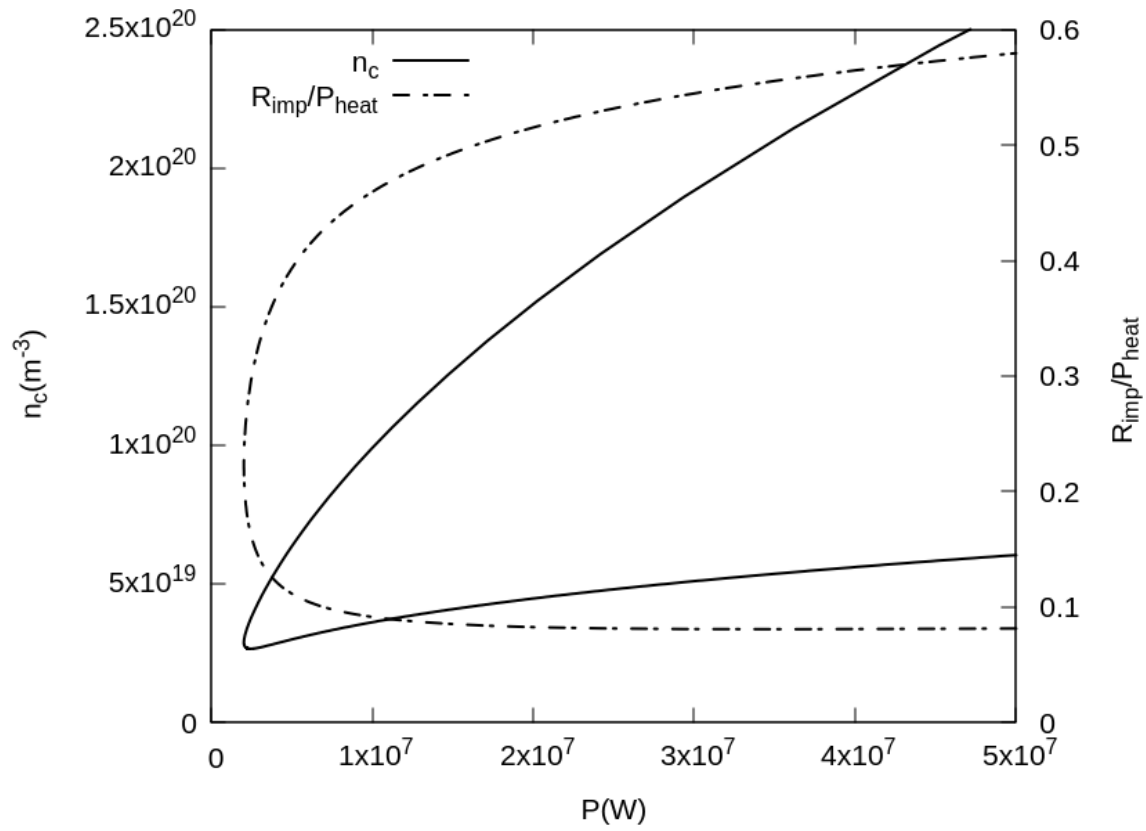


Figure 2. Density limit n_c (solid line) and the radiation to heating power ratio $R_{\text{imp}}/P_{\text{heat}}$ (dashed line) as functions of the heating power P_{heat} with the power and electron density dependence of τ_p in JET experiments as shown in Eq. (13).

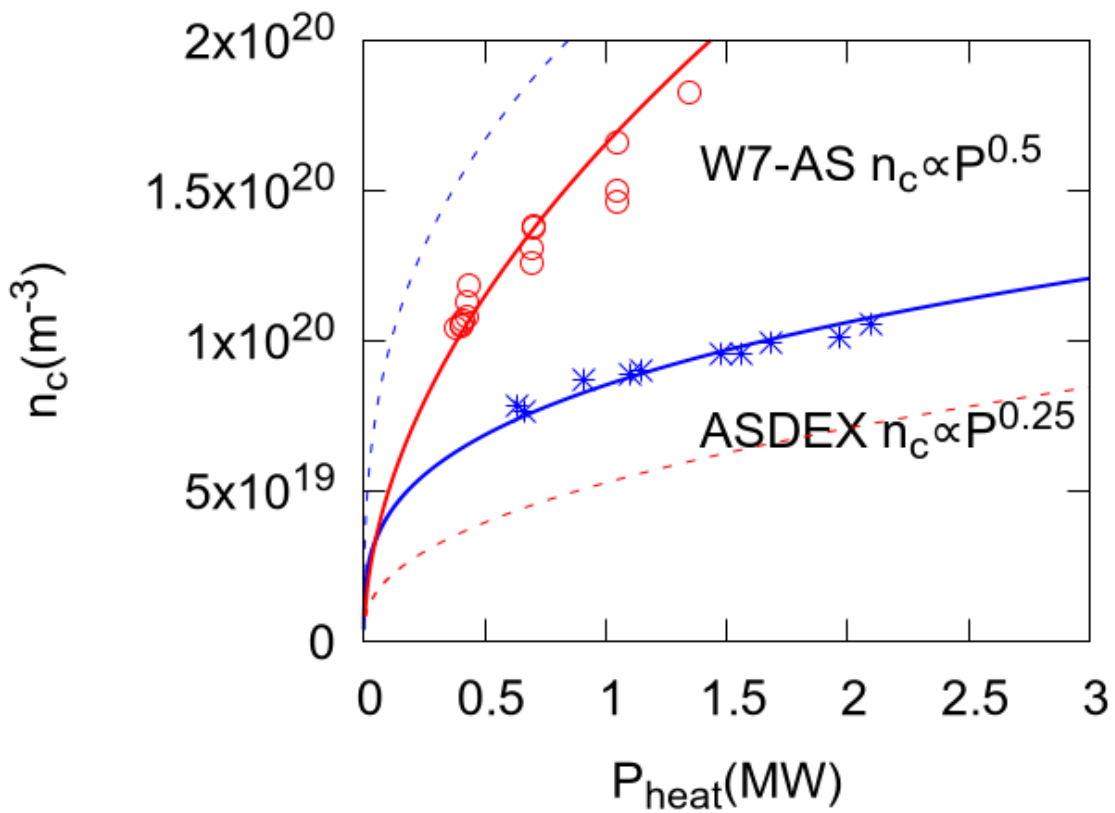


Figure 3. Density limit n_c as functions of heating power P_{heat} from PWSO theory and the experimental data of ASDEX tokamak and W7-AS stellarator considering the sputtering of deuterium on boron and $D_{\perp} = 10^{-2} \text{m}^2/\text{s}$. The experimental and devices' data is taken from [2, 26].

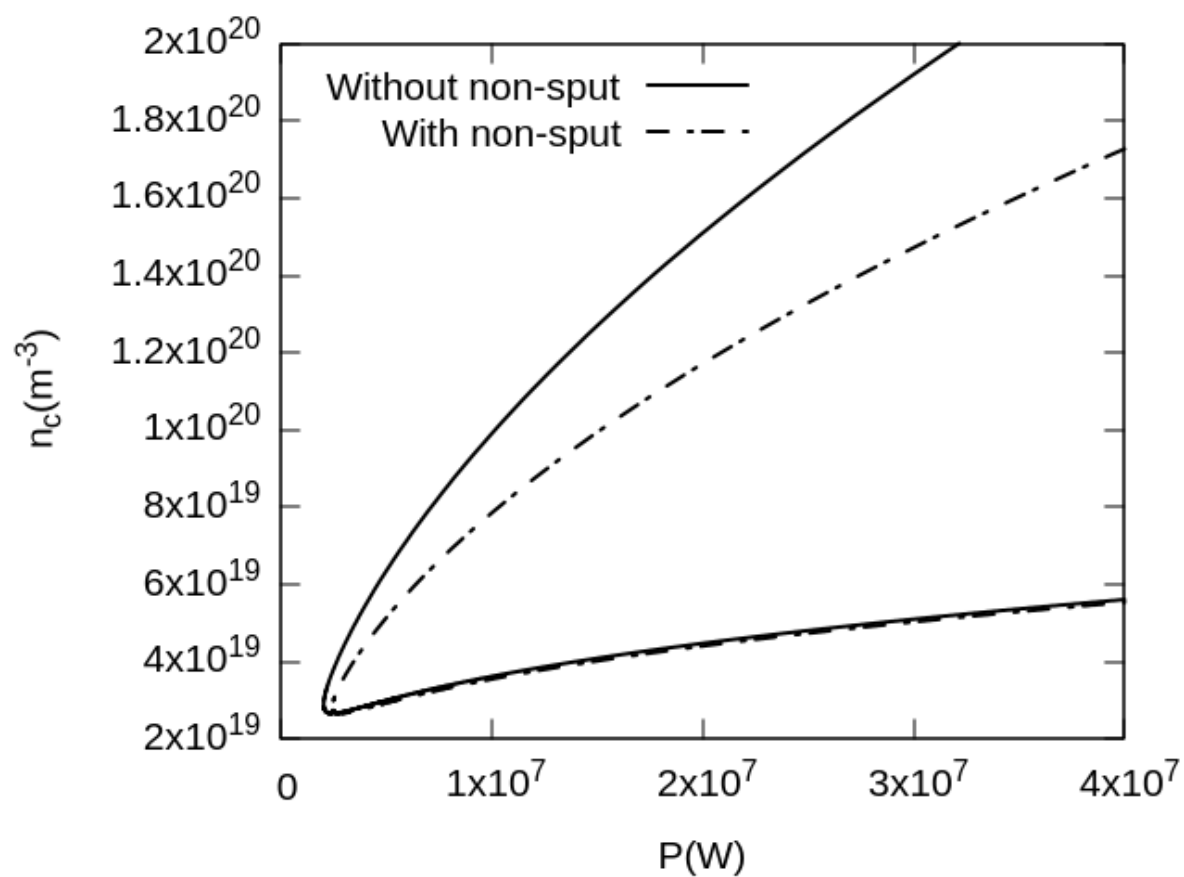


Figure 4. Density limit n_c (solid line) as functions of heating power P_{heat} with (dashed line) and without (solid line) considering the radiation effect due to non-sputtered impurity.

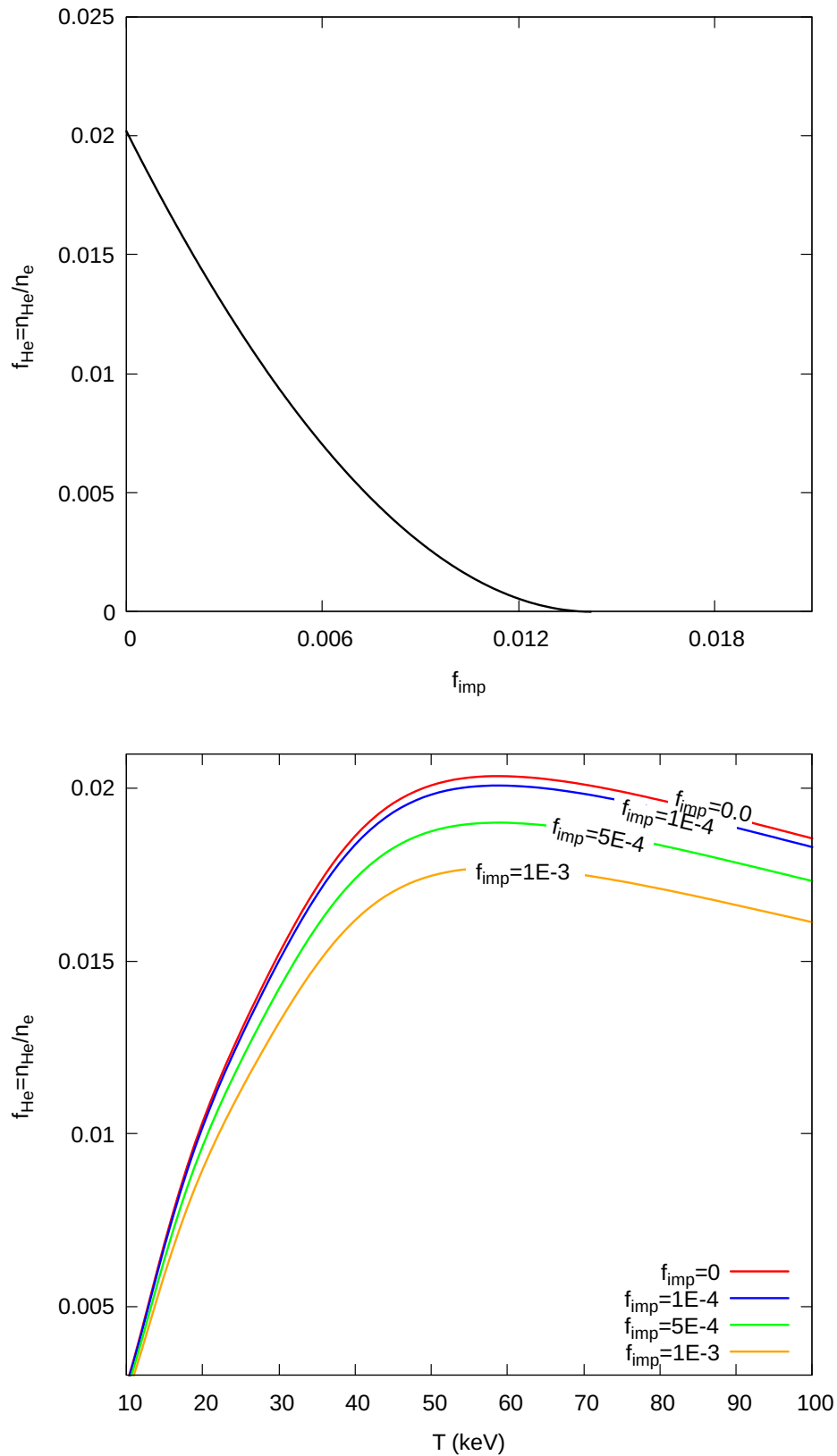


Figure 5. The helium fraction f_{He} as a function of (top) impurity level f_{imp} at the core plasma temperature $T = 51.8$ keV and as functions of (bottom) the core plasma temperature T with various impurity levels at electron density $n_e = 10^{20}\text{m}^{-3}$ and impurity's charge number $Z_{\text{imp}} = 70$.

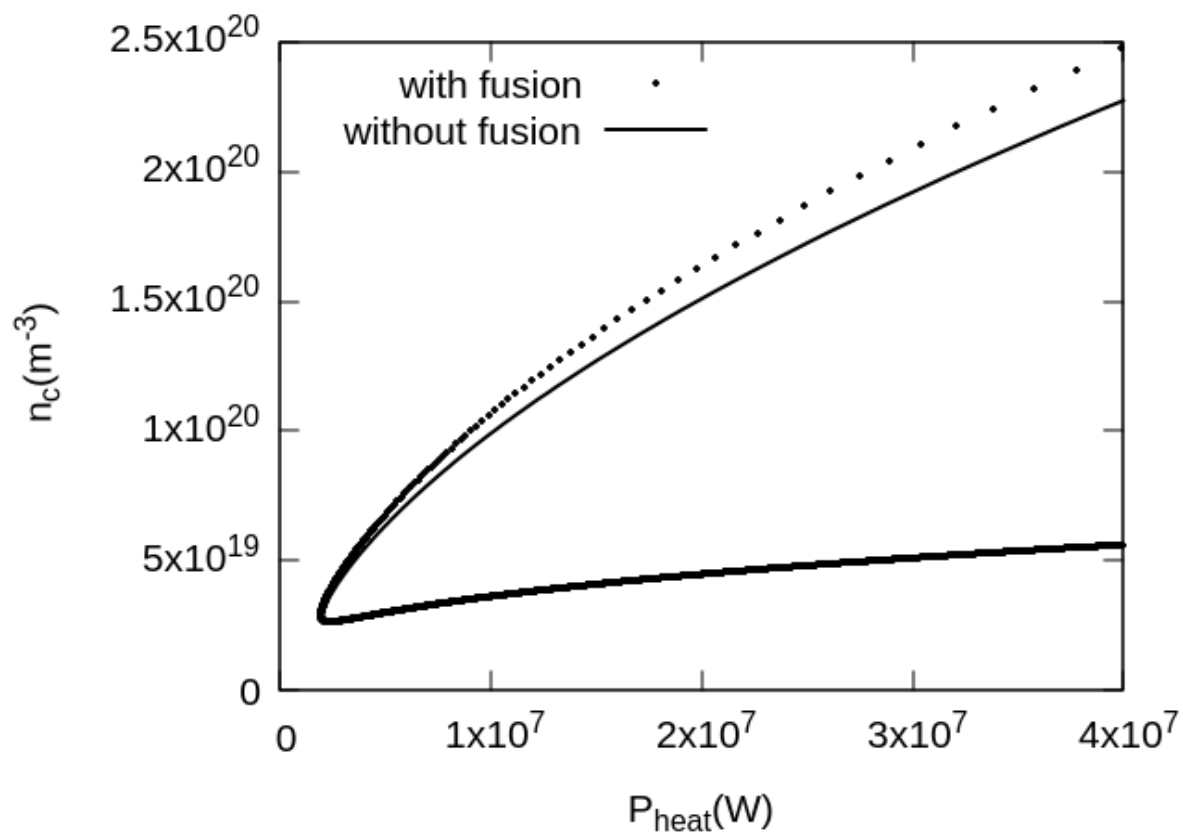


Figure 6. Density limit as functions of heating power P_{heat} (points) with and (solid line) without effects of fusion reactions at plasma temperature $T = 50\text{keV}$.

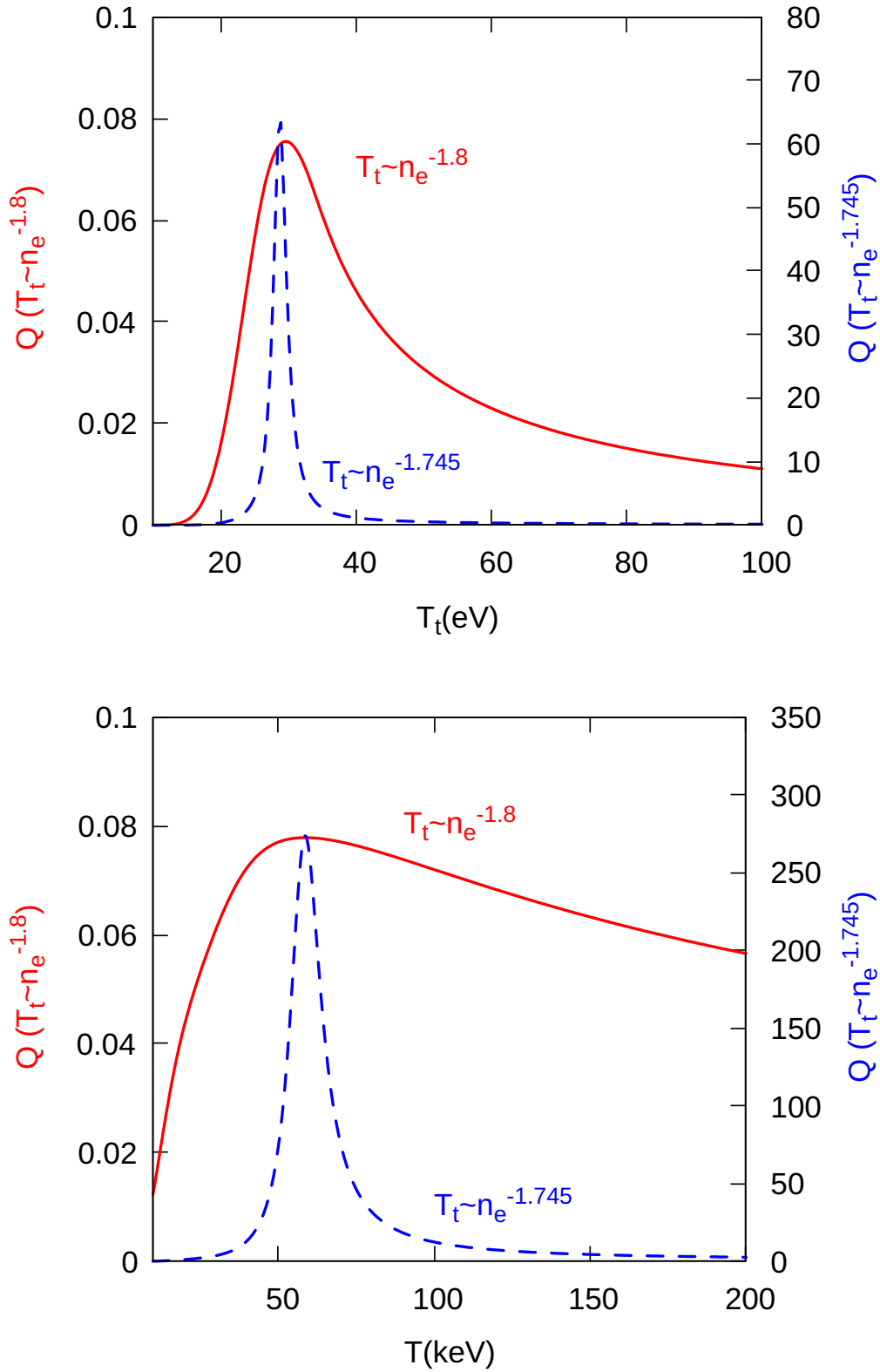


Figure 7. Energy gain factor Q as a function of (top) the target region plasma temperature T_t (eV) at the core plasma temperature $T = 45$ keV and as a function of (bottom) the core plasma temperature T (keV) at $T_t = 30$ eV for (red solid line) the JET τ_p scaling in Eq. (13) and (blue dashed line) the modified τ_p scaling in Eq. (A.1).